Contents lists available at ScienceDirect

Journal of Photochemistry & Photobiology, B: Biology

journal homepage: www.elsevier.com/locate/jphotobiol

Pulsed low-intensity laser treatment stimulates wound healing without enhancing biofilm development *in vitro*

Manuela Besser [a], Lukas Schaeler [b], Isabell Plattfaut [b], Florian H.H. Brill [c], Andreas Kampe [c], Maria Geffken [d], Ralf Smeets [e], E. Sebastian Debus [f], Ewa K. Stuermer [f,*]

[a] *Clinic for General, Visceral and Transplant Surgery, University Hospital Muenster, Germany*
[b] *Institute of Virology and Microbiology, Faculty of Health, Centre for Biomedical Education and Research (ZBAF), Witten/Herdecke University, Germany*
[c] *Dr. Brill + Partner GmbH, Institute for Hygiene and Microbiology, Hamburg, Germany*
[d] *Institute for Transfusion Medicine, University Medical Center Hamburg-Eppendorf, Hamburg, Germany*
[e] *Department of Oral and Maxillofacial Surgery, University Medical Center Hamburg-Eppendorf, Germany*
[f] *Dpt. of Vascular Medicine, University Heart Center, University Medical Center Hamburg-Eppendorf (UKE), Germany*

ARTICLE INFO

ABSTRACT

Objectives: Treating infected or chronic wounds burdened with biofilms still is a major challenge in medical care. Healing-stimulating factors lose their efficacy due to bacterial degradation, and antimicrobial substances negatively affect dermal cells. Therefore, alternative treatment approaches like the pulsed low intensity laser therapy (LILT) require consideration.

Methods: The effect of pulsed LILT (904 nm, in three frequencies) on relevant human cells of the wound healing process (fibroblasts (BJ), keratinocytes (HaCaT), endothelial cells (HMEC), monocytes (THP-1)) were investigated in *in-vitro* and *ex-vivo* wound models with respect to viability, proliferation and migration. Antimicrobial efficacy of the most efficient frequency in cell biological analyses of LILT (3200 Hz) was determined in a human biofilm model (lhBIOM). Quantification of bacterial load was evaluated by suspension method and qualitative visualization was performed by scanning electron microscopy (SEM).

Results: Pulsed LILT at 904 nm at 3200 Hz ± 50% showed the most positive effects on metabolic activity and proliferation of human wound cells *in vitro* (after 72 h – BJ: BPT 0.97 ± 0.05 *vs.* 0.75 ± 0.04 ($p = 0.0283$); HaCaT: BPT 0.79 ± 0.04 *vs.* 0.59 ± 0.02 ($p = 0.0106$); HMEC: 0.74 ± 0.02 *vs.* 0.52 ± 0.04 ($p = 0.009$); THP-1: 0.58 ± 0.01 *vs.* 0.64 ± 0.01 ($p > 0.05$) and *ex vivo*. Interestingly, re-epithelialization was stimulated in a frequency-independent manner. The inhibition of metabolic activity after TNF-α application was abolished after laser treatment. No impact of LILT on monocytes was detected. Likewise, the tested LILT regimens showed no growth rate reducing effects on three bacterial strains (after 72 h - PA: -1.03%; SA: -0.02%; EF: −1,89%) and one fungal (−2.06%) biofilm producing species compared to the respective untreated control. Accordingly, no significant morphological changes of the biofilms were observed after LILT treatment in the SEM.

Conclusions: Frequent application of LILT (904 nm, 3200 Hz) seems to be beneficial for the metabolism of human dermal cells during wound healing. Considering this, the lack of disturbance of the behavior of the immune cells and no growth-inducing effect on bacteria and fungi in the biofilm can be assigned as rather positive. Based on this combined mode of action, LILT may be an option for hard to heal wounds infected with persistent biofilms.

1. Introduction

Medical lasers are divided into two types, the high-intensity laser therapy (HILT) and the low-intensity laser therapy (LILT). Their depth of tissue penetration does not inevitably correlate with the intensity or wavelength, but is rather related to absorption characteristic of the tissue. Both kind of laser differ in three key features, which influence the therapeutic effects: thermal features, which mainly depend on tissue chromophores which absorb specific wavelength, biophysical features such as the wavelength itself, and the mode of application in the form of continuous or pulsed waves. Especially the latter have an impact on tissue relaxation time, which is more valuable for the laser response than

its frequency. In HILT, where the parameters are above the survival threshold, causes an irreversible tissue reaction; therefore, it is applied for vaporization and tissue incision. In contrast, LILT effects are localized within the survival threshold and stimulate tissue regeneration. The type of laser and the irradiation conditions used vary according to the purpose, the patient, and the expected effects of laser treatment. The technology has advanced, and it is known that it does not necessarily need coherent, *i.e.* laser light to stimulate biological processes in the body. There are analyses that indicate devices based on LEDs also show similar results in the improvement of wound healing [1,2]. Therefore, science assigned these treatments to the term "photobiomodulation" (PBM), which was originally coined by the inventor of low-level laser therapy, Endre Mester 1967, and was 2014 from the World Association for Laser Therapy and the North American Association for Light Therapy defined as "*a form of light treatment that utilizes nonionizing forms of light sources, including lasers, light emitting diodes (LEDs) and broadband light, in the visible and infrared spectrum, involving a nonthermal process with endogenous chromophores eliciting photophysical (i.e., linear and nonlinear) and photochemical events at various biological scales*" [3]. It would more closely resemble the way in which we can use it to influence tissue regeneration without any painful interventions [4,5].

Low-intensity laser therapy (LIL) has been shown to promote healing of chronic wounds *in vivo* [6–8] as well as *in vitro* [9–13]. Especially, research has revealed that cell differentiation, proliferation, metabolic activity and subsequent tissue activation were promoted by LILT. It induces cell proliferation [14] and inhibits scar formation [15,16]. Mechanistically, it was shown that the ATP synthesis in the mitochondria is stimulated by the irradiation of skin and wounds with photons during LIL treatment. This leads to a variety of biochemical reactions in the entire body, triggering anti-inflammatory and immunological effects, the stimulation of cell proliferation and improves analgesic function. One prominent application is represented by wavelength between 633 and 690 nm with a dose of 10 J/cm^2 [17–19]. However, there are a multitude of devices with a broad range of wavelengths and doses applying continuous waves (CW) or pulsed laser emission in with various frequencies, which have not been scientifically proved, yet.

This study represents a systematic analysis of the effects of pulsed low intensity laser treatment (904 nm) using three defined frequency spectra on metabolism, proliferation, and migration of the main players of human wound healing in *in-vitro* and *ex-vivo* human wound models. This approach was extended by the examination of possible antibacterial or antifungal effects of these treatment regimes in a novel human plasma biofilm model, because it has been shown, that chronic wounds are burdened with biofilms [20,21]. These biofilms are comprised by multispecies pathogenic bacteria and fungi surrounded by a self-produced extrapolymeric substance (EPS). It was evaluated that the EPS functions as an effective protective shield against antimicrobial therapies [22,23]. Besides possible antimicrobial efficacies, it was essential to exclude possible positive effects on the development of biofilms, before using a biophysical wound therapy that stimulates the cells in chronic wound healing. This question was additionally addressed in this study.

2. Methods

2.1. Cell Cultures and Pulsed Low-Intensity Laser Application

For investigations of the impact of LILT on human cells keratinocytes from a 62-year-old male (HaCaT; CLS Cell Lines Service GmbH, Cat# 300493/p800_HaCaT, RRID:CVCL_0038), skin fibroblasts of newborn foreskin (BJ; ATCC Cat# CRL-2522, RRID:CVCL_3653), human endothelial cells (HMEC, ATCC Cat# CRL 3243) and human monocytes (THP-1, LGC Standards, Wesel, DE) were applied. Keratinocytes and fibroblasts were cultured in DMEM (4.5 g/l D-glucose, 3.7 g/l NaHCO₃; Biochrom GmbH, Berlin, Germany), supplemented with 10% FCS, 1 ng/ml fibroblast growth factor (FGF) and 1 ng/ml epidermal growth factor

(EGF) (both human rec.; PAN-Biotech, Aidenbach, Germany). Endothelial cells were cultured in MCBD131 medium (PAN Biotech, Aidenbach, Germany) supplemented with 10% FCS, 1 μg/ml hydrocortison and EGF/bFGF (1 ng/ml). Monocytes were cultured in RPMI (w: stable Glutamine, w: 2.0 g/l NaHCO3; PAN Biotech, Aidenbach, Germany) supplemented with 10% FCS and 2-mercaptoethanol (0.05 mM; Carl Roth, Karlsruhe, Germany). All cells were kept under humidified conditions with 5% CO_2 at 37C°.

2.2. Metabolic Activity of Human Skin Cells after LIL Application

Viable cells were seeded into 96-well microtiter plates at 4–6×10^3 cells/well and were cultured in a humidified atmosphere at 5% CO_2 and 37 °C. The cells were treated with a pulsed low-intensity laser (904 nm; Bio-Medical-Systems, Wiesbaden, Germany) after 24 h, 48 h and 72 h with a duration of 60 s and in a distance of 1 mm. Three different frequencies programs were applied: 960 Hz −50% (P1), 3200 Hz (P2) and 3200 Hz ±50% (P3). Table 1 summarizes the irradiation parameters of the lasers used at a distance of 1 mm between the addressed object (here: cell culture) and the laser diode as well as 100% amplitude. However, the indicated energy outputs are only computationally correct at constant frequencies: In fact, the laser powers vary as a function of frequency at 960 Hz −50% and 3200 Hz ± 50%, respectively, between the two benchmarks in both directions between 5.5 and 16.2 mW. However, over a longer period, the average values (constant 960 Hz or 3200 Hz) for power and energy can be assumed. The power of a laser pulse is about 22 W with a pulse length of 150 ns.

One hour after laser treatment, the metabolic activity was evaluated by using the CellTiter 96® Aqueous One Solution Cell Proliferation Assay (MTS assay; Promega, Walldorf, Germany) according to manufacturer protocol. - Each analysis was additionally performed in the presence of TNF-α (40 ng/ml; Thermo Fisher Scientific, MA, USA) in the culture medium, mimicking the pro-inflammatory milieu of chronic wounds [24,25].

2.3. Cell Migration of Human Skin Cells under LIL Application

The bottoms of a 24-well cell culture plate were homogeneously coated with 500 μl of rat tail type I collagen ECC LOT 7135002 (Corning B.V., Amsterdam, Netherlands) dissolved in PBS at a concentration of 200 μg/ml, serving as a matrix for the dermal cells. After 2 h, human keratinocytes and endothelial cells (150.000 cells/well) and fibroblasts (175.000 cells/well), were seeded and cultured under humidified conditions. After formation of a confluent monolayer, cultures were incubated with mitomycin (10 μg/ml) for 2 h to prevent further cell proliferation. By using a plastic pipette tip (200 μl), 550 ± 50 μm wide wounds were scratched into the monolayers. The resulting solubilized cells were removed by PBS rinsing, and the cells were subsequently cultured with growth factor-free media. Cell migration was analyzed microscopically (Leica Microsystems, Heerbrugg, Switzerland) over a period of 24 h (fibroblasts, endothelial cells) or 48 h (keratinocytes), respectively. During the above-mentioned period, the cells underwent a laser application of either 960 Hz −50%, 3200 Hz, 3200 Hz ± 50% immediately after scratching and after 8 h post-scratching.

Data analysis was performed manually using the program ImageJ© (Wayne Rasband) including the special wound healing tool and plotted in comparison to the untreated control.

2.4. Human Ex-Vivo Wound Models Based on Abdominoplastic Skin

Human full-thickness skin from surgically removed abdominoplastics (cooperation with plastic surgery) was used to create human *ex-vivo* wound models. The study was approved by the ethic committee of Witten/Herdecke University (Ref.: 84/2017). The full thickness skin was processed before and after sharp removal of the subcutis by two times disinfection with 70% ethanol solution. Using a biopsy punch, 2 mm

Table 1

Irradiation parameters of the pulsed low-intensity laser (904 nm; Bio-Medical-Systems, Wiesbaden, Germany) at 1 mm application distance and 100% amplitude. The mean values for power and energy are indicated within the frequency-dependent range of 5.5 and 16.2 mW. Because the irradiation parameters of the programs P1 (960Hz −50%) and P3 (3200 Hz ±50%) change continuously and without steps between the pulse frequencies 480 Hz to 960 Hz and 1600HZ to 4800 Hz, respectively, the data for the entire range is indicated.

	480 Hz	960 Hz	1600 Hz	3200 Hz	4800 Hz
Frequency [Hz]	480	960	1600	3200	4800
Period length [s]	0.002083333	0.001041667	0.000625	0.0003125	0.000208333
Pulse width [s]	0.00000015	0.00000015	0.00000015	0.00000015	0.00000015
Duty cycle [0…1]	0.000072	0.000144	0.00024	0.00048	0.00072
Amplitude [0…. 1]	1	1	1	1	1
Power (mv) [W]	0.0016	0.0033	0.0055	0.0109	0.0162
Power per pulse [W]	22.71062271	22.91666667	22.91666667	22.70833333	22.5
Time [s]	60	60	60	60	60
Energy [J]	0.186	0.198	0.33	0.654	0.972

wounds were placed in the skin. An 8 mm biopsy punch was then applied to punch out the area around this 2 mm wound to create the *ex-vivo* wound model. Models were positioned in an airlift construct in a 6-well plate filled with 5.5 ml DMEM (containing 3.7 g/l NaHCO3, 4.5 g/l glucose, stable L-glutamine and 10% FCS) per well. During analyzes, media was changed every third day. Adjusted to a possible clinical application laser treatment was performed on day 1, 2, 3, 4, 5, 6, 7, 9, 11 and 13 for 120 s using the above mentioned frequencies. The wounds were collected and fixed on the defined endpoints 5, 10 and 15 days.

2.5. Hematoxylin-Eosin Staining of the Ex-Vivo Wound Models

For subsequent analyses, models were transferred to 4% PFA and fixed automatically over night using an embedding machine (Leica, Bensheim, Germany). The human *ex-vivo* wound models stored in liquid paraffin were cast into blocks using an embedding system (Medite GmbH, Burgdorf, Germany). Paraffin sections (7 μm) were manufactured by using a slide microtome (pfm medical, Nurnberg, Germany). For histology, standard hematoxylin-eosin staining (H/E staining) was performed and evaluated by light microscopy.

2.6. Immunohistochemical Staining of the Ex-Vivo Wound Models

Paraffin sections were deparaffinized and rehydrated by xylene/ethanol washing steps. Immunohistochemical staining to Ki67 was performed to visualize cell proliferation. For antigen retrieval, the slices were heated in 10 mM citrate buffer, pH 6.0 and 0.1% Tween 20 for 20 min, cooled down to room temperature and transferred to $1\times$ phosphate buffered saline (PBS). Permeabilization and blocking of the sections were achieved by incubation with permeabilization buffer containing $1\times$ PBS, 5% goat serum, 5% horse serum and 5% FCS (Pan Biotech) and 0.1% Triton X100 (Merck, Darmstadt, Germany) for 1 h at room temperature (RT). Mouse monoclonal anti human Ki-67 Antigen Clone MIB-1 (Agilent, CA, USA) was diluted 1:50 in blocking solution comprised of $1\times$ PBS, 5% goat serum, 5% horse serum and 5% FCS (Pan Biotech, Aidenbach, Germany) and incubated in a wet chamber at 4 °C over night. After washing with PBS, the Alexa Fluor®488 goat anti-mouse IgG (H + L) (1:500; Life Technologies/Invitrogen) was applied in blocking solution for 1 h at RT. Resting antibody solution was removed by washing with PBS. The sections were embedded in Roti®-Mount FluorCare DAPI (Carl Roth, Karlsruhe, Germany).

The number of proliferating cells was quantified by counting Ki67-immunopositive cells in 3 regions of interests (roi, 10× objective, light microscope (Leica, Wetzlar, Germany)): wound margin left, wound ground, wound margin right on 3 non-consecutive sections of one wound.

2.7. Bacterial Test Organism and Nutrient Solutions

Pseudomonas aeruginosa (DSM-939), Staphylococcus aureus (ATCC 6538) and Enterococcus faecium (ATCC 6057) were cultivated on casein/soy peptone agar plates (CSA). The test yeast *Candida albicans (ATCC 10231)* was cultivated on malt extract agar (MEA) following EN 13727 and EN 13624, respectively. The second subculture was used and bacterial/fungal suspension was adjusted to a 0.5 McFarland standard (approx. 1.5×10^8 cfu/ml) by using a densitometer (Grant Bio™ DEN—1B, Grant Instruments Ltd.; Cambs SG8 6GB, England). Next plasma and buffy coat with donor's immune cells were added. The final bacterial and yeast concentration was set to $1.5–3 \times 10^8$ cfu per single biofilm model. Microbial cfu counts were determined by spreading untreated BTS controls of each experiment onto agar plates to calculate surviving organisms and reduction rates, respectively.

2.8. Leucocyte Rich Human Plasma Biofilm Model (lpBIOM)

The biofilm model lpBIOM used for evaluation of *in vitro* LILT based on fresh frozen plasma (FFP; citrate buffered; blood group AB) and a LRS® chamber of leukocyte apheresis (Trima Accel®, Terumo, USA), containing the "immunocompetence" of the donor. This was gained by using a special Terumo BCT design (Trima Accel® LRS® Platelet, Plasma Set", REF number 82300) which removes nearly all leukocytes of the donor from the platelet sample, so that its concentration is equivalent to about 4×10^4 leukocytes/μl. Blood products were received from the Institute for Transfusion Medicine, UKE, Germany, all donors give their written consent using their blood products and the regulations of "Good clinical practice" were adhered to. Preparation of the models were done as described previously [26,27]. In brief, after thawing FFP it was adjusted to 250 ml and room temperature. The content of one LRS® chamber was placed in a tube, washed with 3 ml of the FFP to remove any residual leukocytes and centrifuged at 1610 *g*. Erythrocytes were gently removed and the remaining plasma-leukocytes mixture was added to the FFP. The bacterial suspension mentioned above was added to this suspension.

2.8.1. Quantitative Evaluation of LIL Effects on the lpBIOM

Twelve hours after preparation of the biofilm models, pulsed LILT with a wavelength of 904 nm and a frequency of 3200 Hz (IDL MP 2510, Bio-Medical-Systems, Wiesbaden, Germany) was applied for the first time followed by a reapplication after 24 h, 48 h and 72 h for 120 s/cm^2 each. This mode of LIL application was chosen because it had the most positive effect on human cells. For analysing LIL effects, 24 h and 72 h models were dissolved using bromelain (Bromelain from pineapple, Serva Electrophoresis GmbH; Heidelberg, Germany). Bromelain solution was prepared using 2.1 g powder, dissolved in 100 ml phosphate buffered saline (PBS) and 1.5 ml was added to each well containing a biofilm model. The biofilm structure was destroyed with sterile pipette tips to ensure complete dissolution of the model within three hours. To quantify the surviving bacteria the resulting solution was serially tenfold diluted. 50 μl of each dilution was plated (spread technique) and incubated for 48 h at 37 °C under aerobic conditions. Colony forming units

(in cfu/ml) were determined using a digital colony counter (NSCA 436000, VWR International GmbH; Germany).

2.8.2. Visualization of LILT Effects on Biofilms by Scanning electron Microscopy (SEM)

To visualize the effects of the LILT on biofilm morphology and structure, scanning electron microscopy (SEM) was performed. lpBIOMs were fixed with a glutaraldehyde/PVP-solution containing 2.5% glutaraldehyde, 2% polyvinylpyrrolidone (PVP) and 0.5% NaNO₂ in 0.1 M cacodylate buffer for 1 h at 4 °C. After washing (3× in 0.1 M cacodylate buffer) models were frozen in liquid nitrogen to get freeze fracture fragments. For glycocalyx staining, samples were incubated for 18 h at RT in an arginin HCl solution (2% arginine-HCL, glycine, sucrose and sodium glutamate). After rinsing three times for 5 min with aqua dest., samples were stored for 5.5 h in a mixture of 2% tannic acid and guanidine-HCl, they were rinsed again, once with aqua dest. (5 min incubation) and three times with 0.1 M Cacodylatbuffer (5 min incubation), followed by an incubation overnight at 4 °C. For staining, samples were placed in a 1% OsO$_4$ solution for 30 min at RT followed by three rinsing steps with 0.1 M cacodylate buffer (10 min incubation) and storing again over night at 4 °C. Samples were dehydrated by an isopropanol series (50%, 70%, 90%, 100%) followed by acetone incubations for 15 min (50%, 75%, 100%). Drying step was then completed by incubation in the critical point dryer (BAL-TEC AG,
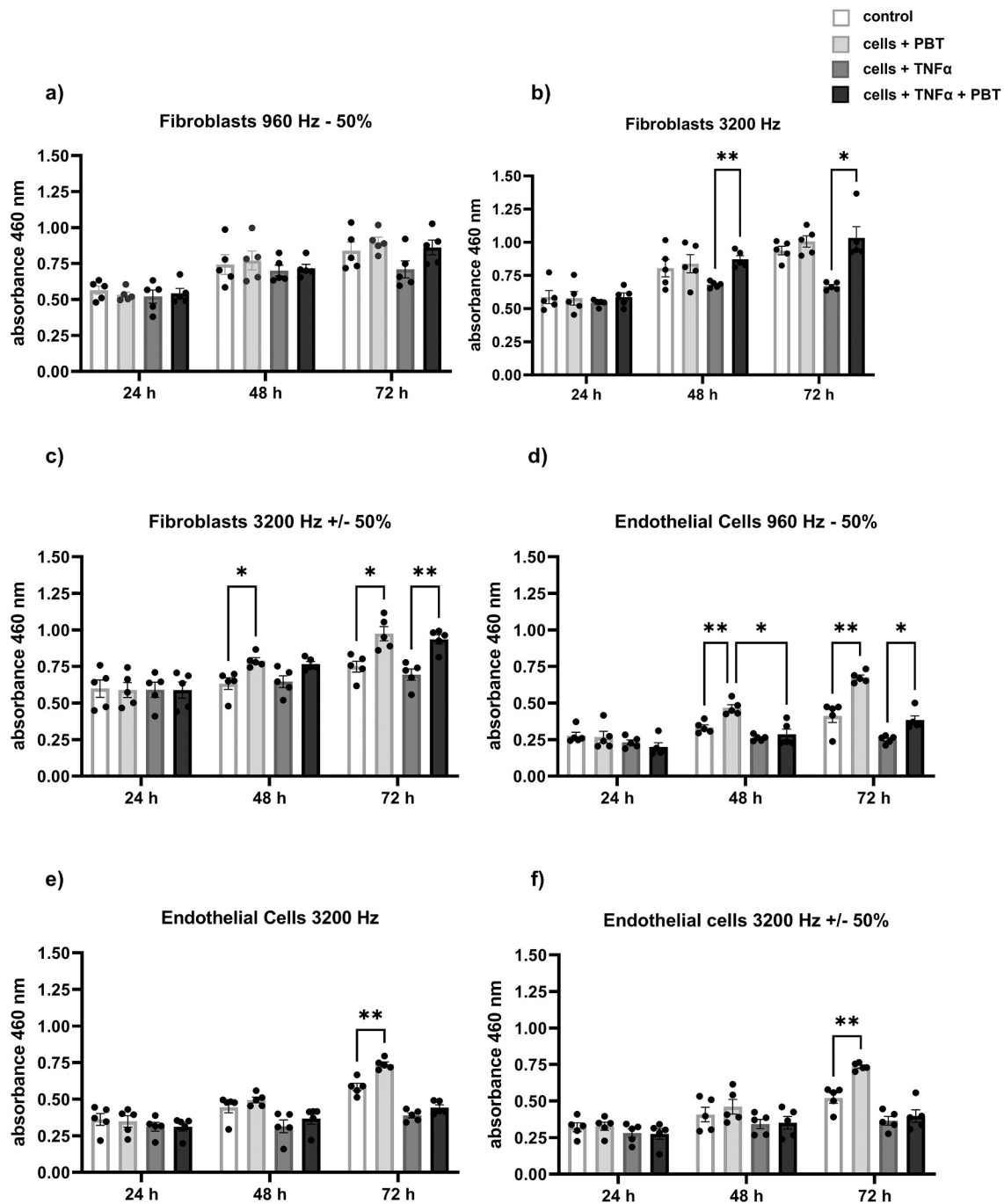

Fig. 1. Metabolic activity of skin fibroblasts (BJ; **a-c**), endothelial cells (HMEC; **d-f**) after 24 h, 48 h and 72 h treatment with pulsed low-intensity laser (904 nm) in three different frequencies with and without TNF-α application. Frequencies were 960 Hz - 50% (**a, d**), 3200 Hz (**b, e**) or 3200 Hz ± 50% (**c, f**). Results are expressed as means ± SEM (*$p \leq 0.05$; **$p \leq 0.01$; ***$p \leq 0.001$: ****$p \leq 0.0001$). Abbreviations: h hour, PBM photobiomodulation, TNF tumor necrosis factor.

Balzers, Liechtenstein). In a last step sample were sputtered (BAL-TEC AG, Balzers, Liechtenstein) with gold palladium and analyzed by Zeiss Sigma VP SEM (Zeiss, Oberkochen, Germany) at 2 kV acceleration voltages using the in lens and SE detectors.

2.9. Statistics

Data are expressed as means ± standard error of the mean (SEM). A *p*-value of $p \leq 0.05$ was considered statistically significant. Cell investigations were performed in triplicates and three-five times independently ($n = 3$; $N = 3-5$). For biofilm evaluation, triplicates each derived of six different anonymous blood donors (FFP and leukocytes) were analyzed. Cell proliferation and migration as well as bacterial

reduction rates (in Δlog10 cfu/ml) were calculated using the statistics program GraphPad PRISM (Version 8.2.1; GraphPad Software Inc., La Jolla, USA). Statistical analysis contained a two-way ANOVA, followed by Holm-Sidak posthoc test for evaluation of multiple comparisons.

3. Results

3.1. Metabolic Activity of Human Skin Cells after LIL Application

In principle, the application of pulsed LIL induced cell type-specific responses in human skin cells. Generally, multiple treatments are more effective, because the results with respect to the metabolic activity of the cells increased in three out of four cell types with ongoing
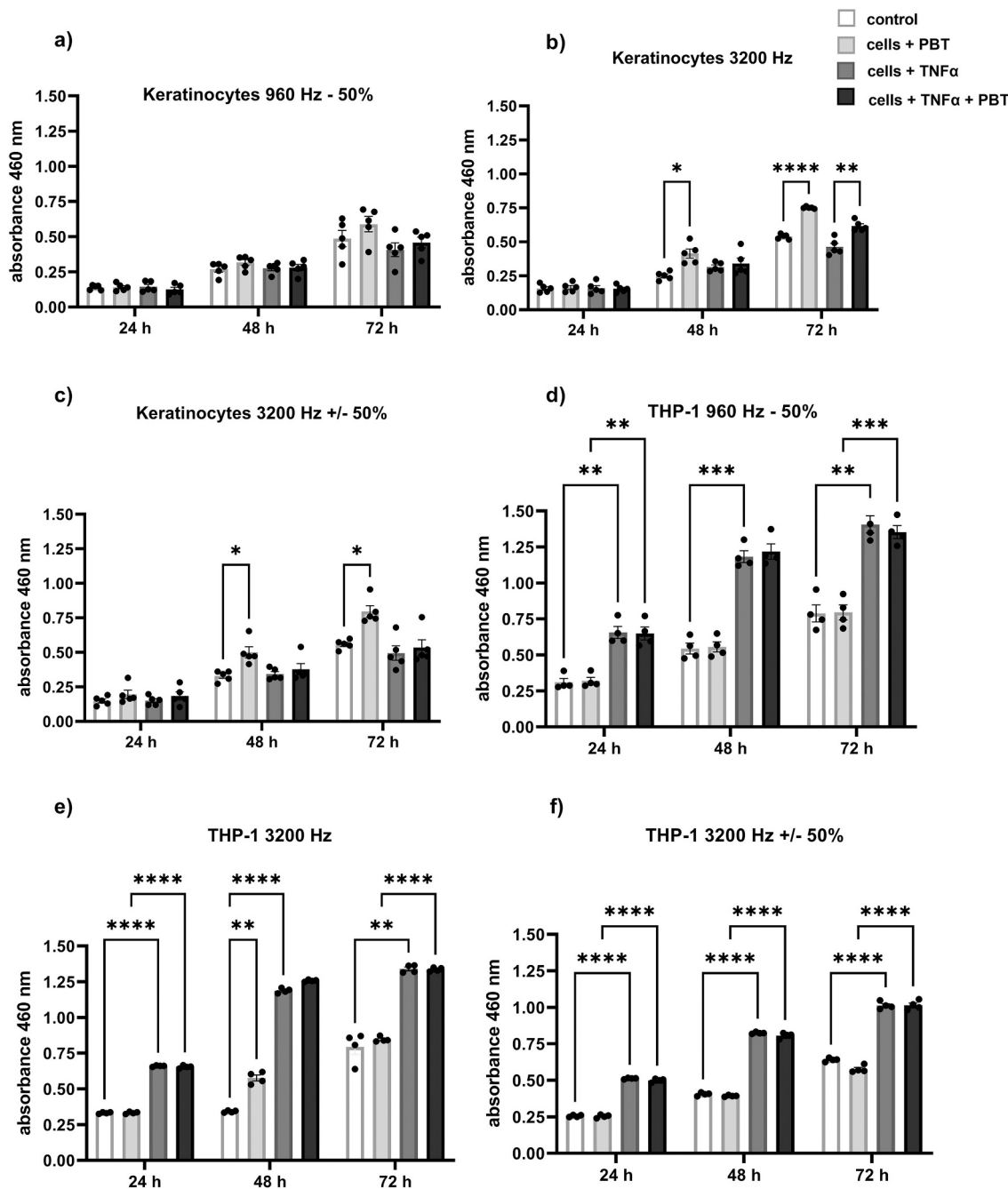

Fig. 2. Metabolic activity of human keratinocytes (HaCaT; **a-c**) and monocytes (THP-1; d-f) after 24 h, 48 h and 72 h treatment with pulsed low-intensity laser (904 nm) in three different frequencies with and without TNF-α application. Frequencies were 960 Hz - 50% (**a, d**), 3200 Hz (**b, e**) or 3200 Hz ± 50% (**c, f**). Results are expressed as means ± SEM (*$p \leq 0.05$; **$p \leq 0.01$; ***$p \leq 0.001$; ****$p \leq 0.0001$). Abbreviations: PBM photobiomodulation, h hour, TNF tumor necrosis factor.

experimental duration (Fig. 1a-f; Fig. 2a-c). This particular effect was most significant in keratinocytes after laser treatment with 3200 Hz and 3200 Hz ±50% (Fig. 2b, c), followed by the significant metabolic enhancement in fibroblasts (Fig. 1b, c). Endothelial cells exclusively displayed the most significant positive effect after the application of lower frequencies 960 Hz −50% (Fig. 1d) compared to the other modi (Fig. 1h, i). Monocytes were not influenced by laser treatment (Fig. 2d-f). The application of the pro-inflammatory cytokine TNF-α into the cell culture medium induced a reduction of the metabolic activities in fibroblasts, endothelial cells and keratinocytes, initiating after 48 h of incubation. The treatment with LIL with the frequencies 3200 Hz and 3200 Hz ± 50% resolved this inhibiting effect especially in human fibroblasts (Fig. 1b, c). A similar effect was determined in keratinocytes, which regenerated their metabolism within 72 h of laser application with 3200 Hz (Fig. 2c). THP-1 monocytes significantly increased their metabolic activity in response to the TNF-α challenge. This physiologically expected reaction was not influenced by laser therapy (Fig. 2d-f).

3.2. Cell Migration of Human Skin Cells under LIL Application

The migration of human fibroblasts in the scratch assay was not affected by laser treatment (Fig. 3b). The application of the laser frequencies 3200 Hz or 960 Hz −50%, respectively, induced a slight tendency of acceleration in endothelial cells (Fig. 3c). However, all scratches were completely closed after 18 h at the latest. The treatment of keratinocytes with the low-intensity laser did not affect the migration behavior within the first 24 h (Fig. 3a). Between 24 h – 48 h, the size of the scratches in the control group increased above 100% due to detaching processes. This effect did not occur by using 3200 Hz or 3200 Hz ± 50%, which inhibited the detachment and stabilised a slow migration of the keratinocytes. At the endpoint of the experiment after 48 h, only 38.75% (3200 Hz) and 36.54% (3200 Hz ± 50%) of the initial scratch area was closed.

3.3. Quantitative Evaluation of Cell Proliferation after LIL Application in the Ex Vivo Wound Model

The immunohistochemical staining to the proliferation marker Ki67 in the *ex-vivo* wound model revealed that the most prominent number of proliferating cells were keratinocytes located at the wound edges of the epidermis (Fig. 4a). The number of immunopositive cells in the dermis was negligible and thus not quantified. Quantitative analysis of Ki67-positive keratinocytes determined a significant increase in the proliferation rate after 10 days LIL therapy with all three frequencies (960 Hz - 50%: $+7.29 \pm 1.75\%$; 3200 Hz: $+6.35 \pm 0.56\%$; 3200 Hz ± 50%: $+5.61 \pm 0.84\%$) (Fig. 4b). This positive effect was further enhanced after 15 days treatment, exclusively by applying the 3200 Hz mode ($+6.62 \pm 1.33\%$). Laser application with frequencies of 960 Hz −50% and 3200

Hz ±50% rather showed a stagnation of keratinocyte proliferation compared to the control and to day 10.

3.4. Histomorphological Evaluation of Wound Closure after LIL Application in the Ex-Vivo Wound Model

H/E-staining of the *ex-vivo* wound models showed significant histological differences dependent on the treatment regime with the pulsed low-intensity laser (Fig. 5). Without any laser therapy, wound closure by epidermal cells was not detected before day 15 of incubation (Fig. 5a, e, i). In contrast, LIL application with all three modi stimulated wound healing, resulting into wound closure after 5 days treatment (Fig. 5b-d). With ongoing regeneration, a frequency-independent increase in thickness and maturation (cornification) of the epidermis was observed (Fig. 5f-h). Wound healing of the dermis was also positively influenced by laser treatment. The progressive structuring was enhanced and the visual tissue integrity was improved especially after the application of LIL with 3200 Hz (Fig. 5g, k) compared to 960 Hz −50% (Fig. 5f, j). The collagen scaffold appeared physiologically aligned and the fibroblasts, migrating in from the wound edges, were homogeneously distributed. Due to the nature of the *ex-vivo* wound model, revascularization events were not proofed.

3.5. Quantitative Evaluation of LILT Effects on the lpBIOM

For the two bacterial species *S. aureus* and *P. aeruginosa* and the fungus *C. albicans* neither stimulatory, nor inhibitory effects on the growth rate was detected after LILT over the study period of 72 h (Fig. 6a, b). In the case of *E. faecium* biofilms, pulsed LIL initially appeared to exert a stimulatory effect (24 h application: (7.92 ± 0.35 $\log_{10}$). This was no longer detected after 72 h (6.88 ± 0.41 $\log_{10}$).

3.6. Morphological Effects of LILT on the lpBIOM Visualized with SEM

Regardless of the pathogen treated with LILT, the biofilm surface was almost entirely closed (Fig. 7). The porosity shown in the SEM was inherent to the biofilm model lhBIOM. Overall, it is noticeable that the surface of the biofilms of *P. aeruginosa* and *C. albicans* (Fig. 7b, d) appears to be rougher, although the individual pathogens were almost completely covered with EPS (small spots under EPS cover). Pulsed LILT was unable to disrupt the biofilm structure, so that no influence on the embedded pathogens was detected in the SEM.

4. Discussion

Photobiomodulation with wavelengths >600 nm reflects the physical application of light. The chosen wavelength of the laser used here was 904 nm to ensure that its light energy is delivered to the body in the
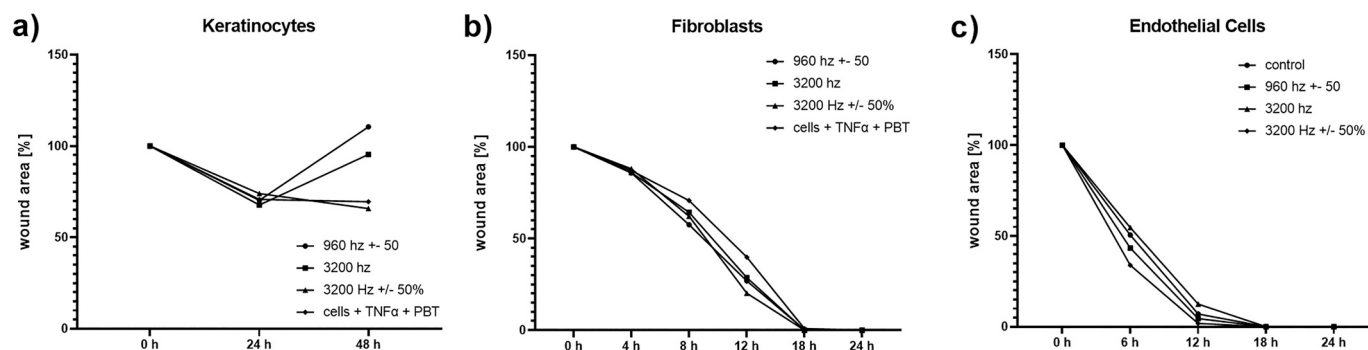

Fig. 3. Results of a scratch assays with human keratinocytes (HaCaT; **a**), skin fibroblasts (BJ; **b**) and endothelial cells (HMEC; **c**), treated with pulsed low-intensity laser (904 nm) with the frequencies of 960 Hz - 50%, 3200 Hz or 3200 Hz ± 50% compared to an untreated control (w/o). Values are expressed as medians and as reduction of the initial scratch area, which was indicated as 100%. (For clarity of presentation, SEM has been omitted.) Abbreviations: w/o without, h hour.
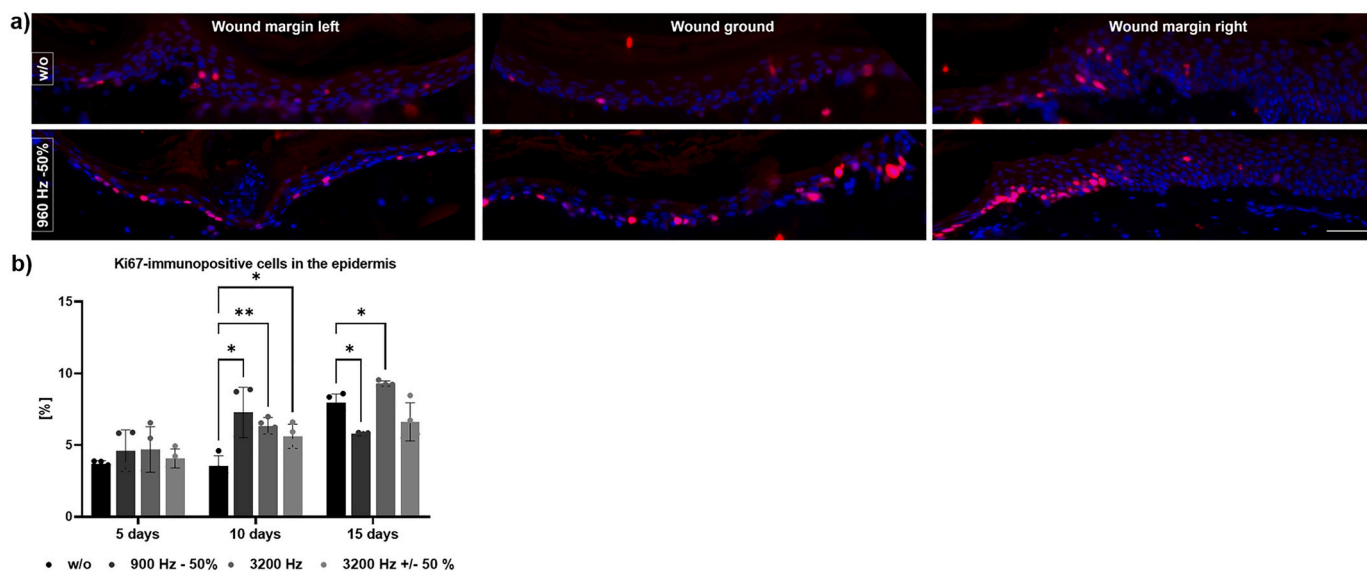
Fig. 4. Proliferation in the human *ex-vivo* wound model. After fixation of the wound models after 5, 10 and 15 days, slices were stained to the proliferation marker Ki67. The number of proliferating cells was quantified by counting Ki67-immunopositive cells in 3 regions of interests (roi, 20× objective): wound margin left, wound ground, wound margin right on 3 non-consecutive sections of one wound. Results are expressed as means ± SEM (*$p \leq 0.05$; **$p \leq 0.01$; ***$p \leq 0.001$: ****$p \leq 0.0001$). Abbreviations: w/o without.
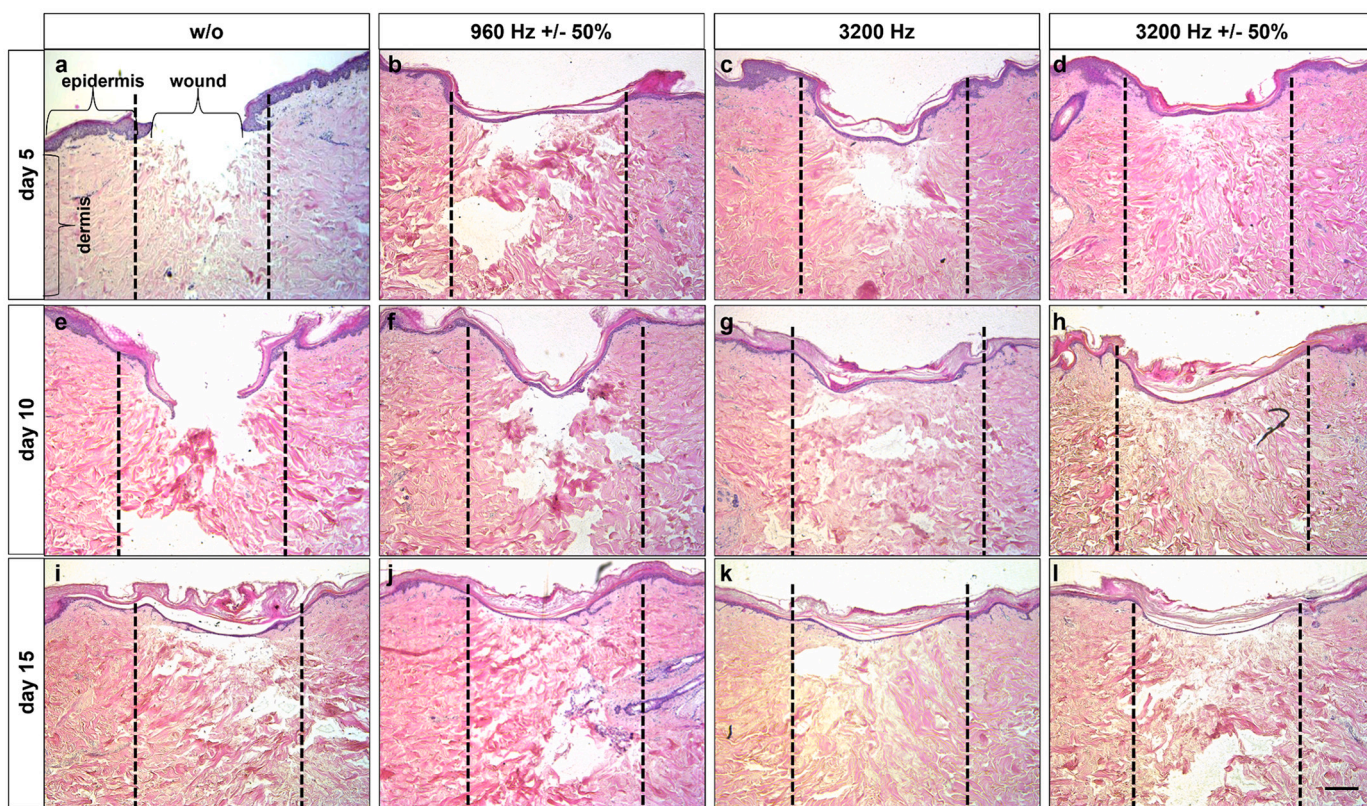

Fig. 5. Histomorphological analysis of wound healing in the *ex-vivo* model by means of H/*E*- staining of sections after 5-, 10- and 15-days post-wounding. Dotted lines represent the wound area. Scale bar = 100 μm; Abbreviations: w/o without.

form of photons to act on the chromophores that can enhance or activate chemical reactions. The skin provides a kind of "window" in the wavelength interval between 600 and 1000 nm and allows the highest transmission and thus penetration depth of the laser light in this range. Its therapeutic application is mainly established in the veterinary medicine and in human complementary medicine today. Indications include pain syndromes, inflammations, but also the induction and improvement of wound healing processes in acute and chronic wounds. The therapeutic value of low intensity laser treatment is discussed differentially in the literature. This is probably due to the lack of consensus on standardized treatment parameters such as wavelength, dose and duration, preventing direct comparison and consistent protocol
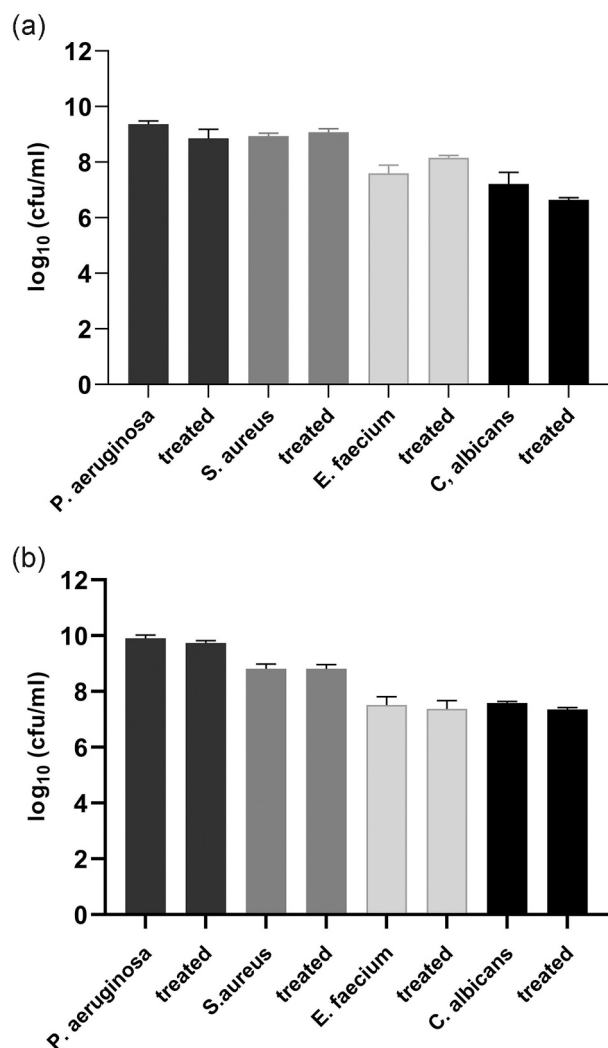
Fig. 6. Comparison of low level laser treatment (LILT) on biofilm models (lhBIOM) of *P.aeruginosa*, *S. aureus, E. faecium* and the fungi *C. albicans*. **a** Results after 24 h of regular growth and single application of laser. **b** Reduction rates of included bacteria or fungi (in log_{10} cfu/ml) are outlined over the course of 72 h of LIL treatment of biofilm growth. Values expressed as mean ± SEM.

recommendations for clinical guidelines. Some studies, reviewed by [19], explained that the effect of low intensity laser is based on stimulating positive subcellular mechanisms. To achieve this effect, the LILT used here operates with pulsations in the frequency bands 960 Hz −50% and 3200 Hz ± 50%, *i.e.* from a technical point of view continuously and without steps in the rages 480 Hz to 960 Hz and 1600 Hz to 4800 Hz, respectively (Table 1). With these ranges, a sufficient depth should always be achieved, even with heterogeneous tissue compositions (individual or contemporaneous conditioning of tissues or cells). However, due to the many differently used parameters of LILT, the current data does not allow a reliable definition of specific frequencies. Thus, it remains unclear whether the pulsed laser is superior to the continuous wave laser or *vice versa*. In contrast other studies postulate therapeutic effects to be traced back to a placebo effect [28,29]. However, with respect to the successful therapies using photobiomodulation in equines and other animal studies, sole placebo effects can be excluded [30–33]. Therefore, getting more scientific experience and knowledge of the efficacy and underlying physiological mechanisms is still essential.

4.1. Skin Cell Response to LIL Application

This study comprises a systematic analysis of pulsed low intensity laser treatment using different frequency spectra on human keratinocytes, fibroblasts, endothelial cells and monocytes with a focus on effects on wound healing processes in *in-vitro* and human *ex-vivo* wound models. It was astonishing and has to be emphasized that laser treatment induced cell type-, time - and frequency-specific effects. For instance, in the human *ex-vivo* wound model, a significant increase in cell proliferation, particularly in the epidermis, was determined after 10 days laser therapy using a wide spectrum between 450 and 5000 Hz (Fig. 4). Human fibroblasts were also positively affected (Fig. 1). With respect to the pulsation, the most outstanding newly discovered candidate, which progressively improved the wound healing efficacy in terms of enhancement of metabolic activity and proliferation of keratinocytes and fibroblasts as well as the development of tissue integrity can be assigned to the treatment with 3200 Hz. Similar results together with an increased expression of Cyclin D1 were described on HaCat cell cultures treated with a 660 nm constant laser light [34]. Recently, it was shown, that a constant application of 980 nm laser light induces microvesicles release in human keratinocytes in a PI3-kinase dependent pathway [35]. Further studies combining different wavelength and pulsation with 3200 Hz would be interesting to assess possible synergistic effects. These regimes might be considered for the treatment of acute and chronic wounds to improve or even re-activate wound healing processes.

Furthermore, endothelial cells showed the most significant effects in response to the application of 960 Hz −50% *in vitro* (Fig. 1d-f). This effect was described for other human endothelial cells (HECV) and could be assigned to an increase of reactive oxygen species production. However, an 808 nm device without pulsation has been applied [36]. Despite the fact, that these results are exclusively based on an *in-vitro* monolayer model and further studies must follow, for the translational clinical approach, this should be kept in mind to consider the stimulation of neovascularization in chronic wounds, lacking appropriate tissue perfusion, for instance due to macro- or microangiopathies (PAOD, diabetes mellitus). Some animal studies on rats determined inhibitions of inflammatory responses and improved healing of burn wounds by means of superpulsed low-level-laser therapy with 904 nm and 100 Hz [37,38]. Also, the cutaneous wound healing in diabetic rats was enhanced after application of 632 nm constant light [39]. Regarding possible biochemical reactions, which might be influenced by laser treatment, Fuchs et al. 2021 postulate, that laser application induces modulations of the cellular responses by stimulating the ATP production, leading to a slightly increased production of hydrogen peroxide (H_2O_2) in the mitochondria accompanied by improved viability and enhanced proliferation [40].

TNF-α is often used to mimic a stress or pro-inflammatory response in cells *in vitro* [24,41]. In this study, the TNF-α challenge induced a significant reduction of the metabolic activities of fibroblasts, keratinocytes and endothelial cells with increasing incubation time (Figs. 1, 2). In the case of fibroblasts and keratinocytes, it was determined that the application of the low intensity laser at 3200 Hz results in a significant reduction of the negative effect on cell viability after 48 h or 72 h, respectively. This protective effect could be based on a published reduction of the pro-inflammatory mediators cyclooxygenase 2 (Cox2), interleukin-6 (IL-6) and tumor necrosis factor-α (TNF-α) [37,42], which was assigned to be potential laser-induced mechanisms, triggering the positive effects on viability and proliferation of fibroblasts, evaluated in this study. As physiologically expected, the monocytes THP-1 responded to TNF-α application with a significant and time-independent enhancement of their metabolic activity, which was not interfered by laser treatment. This knowledge is very important and enables the exclusion of adverse effects, for instance the induction of uncontrolled proliferation of pro-inflammatory monocytes, leading to chronic inflamed wound milieus accompanied with inhibited wound healing. Another adverse effect, *vice-versa*, would be a decrease of the
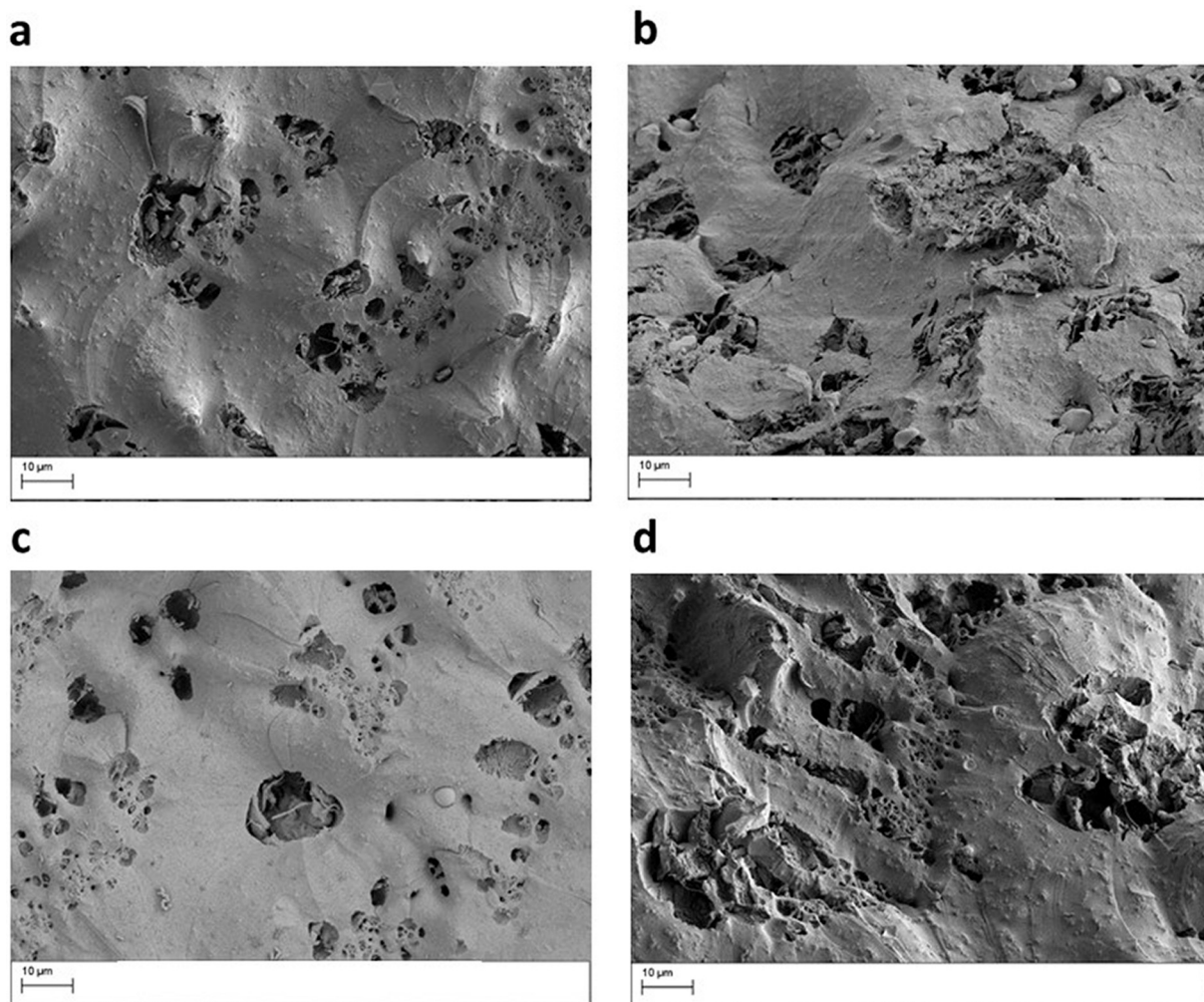
Fig. 7. Scanning electron microscopy (SEM) visualization of biofilm surface alteration in the lhBIOM of *P.aeruginosa* PE **a** *S. aureus* **b** *E. faecium* **c** and the fungi *C. albicans* **d** and after 72 h and three times application of the low-level laser. In all biofilms, LILT seemed not to harm the EPS of biofilm so that it looks smooth. The porosity did not differ to the untreated control so that the "resistance" to laser application was visible.

physiologically normal metabolic activity, also inducing a disturbed wound healing and inhibited immune competence to manage bacterial infections. Both can be excluded know. In progressive examinations, it would be interesting to evaluate effects on pathologically active macrophages.

4.2. Bacterial Colonization and Wound Biofilm under LIL Application

In contrast to near infrared laser, in many studies the short-wavelength blue light (400–480 nm) has been shown to have an eradicating effect on bacteria but, simultaneously, are harmful to the cells [43–45]. For long-wave photobiomodulation therapy, however, the situation is reversed [43,46,47]: While predominantly positive effects on skin cells and their wound healing are described for LILT with a frequency above 635 nm [48,49], the results in research groups differ considerably about an antibacterial efficacy. Various *in vivo* studies have shown that LILT with a wavelength of 808 nm stimulates normal wound healing as well as that of infected wounds [50–52]. However, the results of trials on LILT are difficult to compare because the treatment regimens differ in duration and intensity. A longer treatment and extended therapy have been shown to be beneficial for LILT outcome. This study analyzed possible antimicrobial effect on *S. aureus, P. aeruginosa, E. faecium,* and *C. albicans* in a novel human plasma biofilm model after pulsed low intensity laser application. A 904 nm laser was used, and

three different frequency spectra applied (960 Hz – 50%, 3200 Hz, 3200 Hz ± 50%). The development of the biofilms where neither positively nor negatively influenced in all treatment approaches. Nevertheless, there are promising results after combining photosensitizer and low intensity laser (665 nm) in the successful eradication of different *Staphylococcus* species, *Pseudomonas aeruginosa* and *Acinetobacter baumannii* [53,54]. This combination will be investigated in progressing studies with the tested regimes in this study.

Moreover, it is also essential to register, that no adverse effect in the form of enhanced bacterial growth was determined. This is especially important to know for the treatment of biofilm-burdened chronic wounds: improving effect on wound healing, while exclusion of growth-promoting activity of bacterial growth rate.

5. Conclusions

The pulsed low intensity laser therapy with a 904 nm laser devices and different pulsation regimes applied here induced celltype-, time - and frequency-specific effects on metabolic activity and proliferation of human wound cells in *in-vitro* and *ex-vivo* models. In particular, at a frequency of 3200 Hz, it stimulates fibroblasts and keratinocytes. Endothelial cells were more significantly influenced by 960 Hz −50% LIL. Frequent application seems to be beneficial. No effect was detected on monocytes, represented here by THP-1 cells. Thus, monocytes retain

their physiological activity. Likewise, LILT displayed no antimicrobial activities in this study set-up. In combination with the cell biological results, this is obviously positive, because there is no stimulation of bacterial/fungal metabolism or proliferation.

The new knowledge about enhancing the positive effects of laser treatment, simply by pulsed application with different frequencies, emphasizes the fine and precise biological responses to this therapy. This is often postulated to be negative, because of the difficulty to create consistent guidelines. On the other side, the trend of medical interventions is moving in the direction of individualized therapies. After performing a detailed differential diagnostic, the generation of patient-specific treatment regimens will be possible, provided by the knowledge of the finetuning potential of photobiomodulation therapy. Furthermore, the effects should be compared to the application of continous wave laser mode in follow-up studies.

Funding

Declaration of Competing Interest

All authors declare no conflict of interest.

Acknowledgments

References

[1] M.E. Chaves, A.R. Araújo, A.C. Piancastelli, M. Pinotti, Effects of low-power light therapy on wound healing: LASER x LED, Ann Bras Dermatol. 89 (2014) 616–623, https://doi.org/10.1590/abd1806-4841.20142519.

[2] P. Dungel, J. Hartinger, S. Chaudary, P. Slezak, A. Hofmann, T. Hausner, M. Strassl, E. Wintner, H. Redl, R. Mittermayr, Low level light therapy by LED of different wavelength induces angiogenesis and improves ischemic wound healing, Lasers Surg. Med. 46 (2014) 773–780, https://doi.org/10.1002/lsm.22299.

[3] R.C. Mosca, A.A. Ong, O. Albasha, et al., Photobiomodulation therapy for wound care: a potent, noninvasive, photoceutical approach, Adv. Skin Wound Care 32 (2019) 157–167, https://doi.org/10.1097/01.ASW.0000553600.97572.d2.

[4] M.R. Hamblin, Photobiomodulation or low-level laser therapy, J. Biophotonics 11-12 (2016) 1122–1124, https://doi.org/10.1002/jbio.201670113.

[5] H. Walter, A. Walter, Photobiological basics of low-level-laser-application, In: DZA 2 (1997).

[6] A. Schindl, G. Heinze, M. Schindl, et al., Systemic effects of low-intensity laser irradiation on skin microcirculation in patients with diabetic microangiopathy, Microvasc. Res. 64 (2002) 240–246.

[7] A. Kaviani, G.E. Djavid, L. Ataie-Fashtami, et al., A randomized clinical trial on the effect of low-level laser therapy on chronic diabetic foot wound healing: a preliminary report, Photomed. Laser Surg. 29 (2011) 109–114, https://doi.org/10.1089/pho.2009.2680.

[8] Y. Zhou, H.W.A. Chia, H.W.K. Tang, S.Y.J. Lim, et al., Efficacy of low-level light therapy for improving healing of diabetic foot ulcers: A systematic review and meta-analysis of randomized controlled trials, Wound Repair Regen. 29 (2021) 34–44, https://doi.org/10.1111/wrr.12871.

[9] A.F. Do Soccoro, R.M. Clark, L.M. Ferreira, Effects of low-level laser therapy on wound healing, Rev. Col. Bras. Cir. 41 (2014) 129–133, https://doi.org/10.1590/s0100-69912014000200010.

[10] L. Dancáková, T. Vasilenko, I. Kováč, et al., Low-level laser therapy with 810 nm wavelength improves skin wound healing in rats with streptozotocin-induced diabetes, Photomed. Laser Surg. 32 (2014) 198–204, https://doi.org/10.1089/pho.2013.3586.

[11] P.T.R. de Abreu, J.A.A. de Arruda, R.A. Mesquita, et al., Photobiomodulation effects on keratinocytes cultured in vitro: a critical review, Lasers Med. Sci. 34 (2019) 1725–1734, https://doi.org/10.1007/s10103-019-02813-5.

[12] M.D. Martins, F.M. Silveira, M.A.T. Martins, et al., Photobiomodulation therapy drives massive epigenetic histone modifications, stem cells mobilization and accelerated epithelial healing, J. Biophotonics 7 (2020), e202000274, https://doi.org/10.1002/jbio.202000274.

[13] E. Rahbar Layegh, F. Fadaei Fathabadi, M. Lotfinia, et al., Photobiomodulation therapy improves the growth factor and cytokine secretory profile in human type 2 diabetic fibroblasts, J. Photochem. Photobiol. B 210 (2020), 111962, https://doi.org/10.1016/j.jphotobiol.2020.

[14] R. Fekrazad, S. Asefi, M. Allahdadi, K.A. Kalhori, Effect of photobiomodulation on mesenchymal stem cells, Photomed. Laser Surg. 34 (2016) 533–542, https://doi.org/10.1089/pho.2015.4029.

[15] M.M. Khedr, W.H. Mahmoud, F.A. Sallam, N. Elmelegy, Comparison of Nd: YAG laser and combined intense pulsed light and radiofrequency in the treatment of hypertrophic scars: A prospective clinico-histopathological study, Ann. Plast. Surg. 84 (2020) 518–524, https://doi.org/10.1097/SAP.0000000000002086.

[16] F. Ansari, F. Sadeghi-Ghyassi, B. Yaaghoobian, The clinical effectiveness and cost-effectiveness of fractional CO2 laser in acne scars and skin rejuvenation: A meta-analysis and economic evaluation, J. Cosmet. Laser Ther. 20 (2018) 248–251, https://doi.org/10.1080/14764172.2017.1400173.

[17] F.A.H. Al-Watban, X.Y. Zhang, B.L. Andres, Low-level laser therapy enhances wound healing in diabetic rats: a comparison of different lasers, Photomed. Laser Surg. 25 (2007) 72–77, https://doi.org/10.1089/pho.2006.1094.

[18] F.S. Andrade, R.M. Clark, M.L. Ferreira, Effects of low-level laser therapy on wound healing rev, Col. Bras. Cir. 41 (2014) 129–133, https://doi.org/10.1590/s0100-69912014000200010.

[19] D. Tata, R.W. Waynant, Laser therapy: A review of its mechanism of action and potential medical applications, Laser Photonics Rev. 5 (2011) 1–12, https://doi.org/10.1002/lpor.200900032.

[20] P.G. Bowler, B.I. Duerden, D.G. Armstrong, Wound microbiology and associated approaches to wound management, Clin. Microbiol. Rev. 14 (2001) 244–269.

[21] G.A. James, E. Swogger, R. Wolcott, et al., Biofilms in chronic wounds, Wound Repair Regen. 16 (2008) 37–44.

[22] M. Besser, M. Dietrich, L. Weber, et al., Efficiency of antiseptics in a novel 3-dimensional human plasma biofilm model (hpBIOM), Scientific Rep. Nature Res. 10 (2020) 4792, https://doi.org/10.1038/s41598-020-61728-2 4.

[23] J.D. Rembe, L. Huelsboemer, M. Besser, E.K. Stuermer, Anti-biofilm activity of antimicrobial hypochlorous wound irrigation solutions compared to common wound antiseptics and bacterial resilience in a novel in-vitro human plasma biofilm model (hpBIOM), Front. Microbiol. 11 (2020), 564513.

[24] M.V. Mendez, J.D. Raffetto, T. Phillips, et al., Menzoian, the proliferative capacity of neonatal skin fibroblasts is reduced after exposure to venous ulcer wound fluid: A potential mechanism for senescence in venous ulcers, J. Vasc. Surg. 30 (1999) 734–743, https://doi.org/10.1016/S0741-5214(99)70113-8.

[25] M.W. Loeffler, H. Schuster, S. Bühler, S. Beckert, Wound fluid in diabetic foot ulceration: more than just an undefined soup? Int J Low Extrem Wounds 12 (2013) 113–129, https://doi.org/10.1177/1534734613489989.

[26] E.K. Stuermer, I. Plattfaut, M. Besser, et al., Comparative analysis of biofilm models to determine the efficacy of antimicrobials, J. Hygiene Environ. Health 234 (2021), 113744.

[27] E.K. Stuermer, I. Plattfaut, M. Dietrich, et al., In vitro activity of antimicrobial wound dressings on P. aeruginosa wound biofilm, Front. Microbiol. 12 (2021), 664030.

[28] A.K. Røynesdal, T. Björnland, P. Barkvoll, H.R. Haanaes, The effect of soft-laser application on postoperative pain and swelling. A double-blind, crossover study, J. Oral Maxillofac. Surg. 22 (1993) 242–245.

[29] S. Fernando, A randomised double blind comparative study of low level laser therapy following surgical extraction of lower third molar teeth, Br. J. Oral Maxillofac. Surg. 31 (1993) 170–172.

[30] C. Mignon, N.E. Uzunbajakava, B. Raafs, N.V. Botchkareva, D.J. Tobin, Photobiomodulation of human dermal fibroblasts in vitro: decisive role of cell culture conditions and treatment protocols on experimental outcome, Sci. Rep. 7 (2017) 2797, https://doi.org/10.1038/s41598-017-02860-z.

[31] I. Khan, S.U. Rahman, E. Tang, et al., Accelerated burn wound healing with photobiomodulation therapy involves activation of endogenous latent TGF-β1, Sci. Rep. 11 (2021) 13371, https://doi.org/10.1038/s41598-021-92650-w.

[32] A. Moradi, F. Zare, A. Mostafavinia, et al., Photobiomodulation plus adipose-derived stem cells improve healing of ischemic infected wounds in type 2 diabetic rats, Sci. Rep. 10 (2020) 1206, https://doi.org/10.1038/s41598-020-58099-z.

[33] N.H. Houreld, S.M. Ayuk, H. Abrahamse, Cell adhesion molecules are mediated by Photobiomodulation at 660 nm in diabetic wounded fibroblast cells, Cells 7 (2018) 30, https://doi.org/10.3390/cells7040030.

[34] F.F. Sperandio, A. Simões, L. Corrêa, et al., Low-level laser irradiation promotes the proliferation and maturation of keratinocytes during epithelial wound repair, J. Biophotonics 8 (2015) 795–803, https://doi.org/10.1002/jbio.201400064.

[35] F. Lovisolo, F. Carton, S. Gino, et al., Photobiomodulation induces microvesicle release in human keratinocytes: PI3 kinase-dependent pathway role, Lasers Med. Sci. 7 (2021), https://doi.org/10.1007/s10103-021-03285-2.

[36] A. Amaroli, S. Ravera, F. Baldini, et al., Photobiomodulation with 808-nm diode laser light promotes wound healing of human endothelial cells through increased reactive oxygen species production stimulating mitochondrial oxidative phosphorylation, Lasers Med. Sci. 34 (2019) 495–504, https://doi.org/10.1007/s10103-018-2623-5.

[37] A. Gupta, G.K. Keshri, A. Yadav, et al., Superpulsed (Ga-As, 904 nm) low-level laser therapy (LLLT) attenuates inflammatory response and enhances healing of burn wounds, J. Biophotonics 8 (2015) 489–501, https://doi.org/10.1002/jbio.201400058.

[38] A. Yadav, S. Verma, G.K. Keshri, A. Gupta, Role of 904 nm superpulsed laser-mediated photobiomodulation on nitroxidative stress and redox homeostasis in burn wound healing, Photodermatol. Photoimmunol. Photomed. 36 (2020) 208–218, https://doi.org/10.1111/phpp.12538.

[39] K.R. Byrnes, L. Barna, V.M. Chenault, et al., Photobiomodulation improves cutaneous wound healing in an animal model of type II diabetes, Photomed. Laser Surg. 22 (2004) 281–290, https://doi.org/10.1089/pho.2004.22.281.

[40] C. Fuchs, M.S. Schenk, L. Pham, et al., Photobiomodulation response from 660 nm is different and more durable than that from 980 nm, Lasers Surg. Med. 53 (2021) 1279–1293, https://doi.org/10.1002/lsm.23419.

[41] B. Bucalo, W.H. Eaglstein, V. Falanga, Inhibition of cell proliferation by chronic wound fluid, Eur. Tissue Repair. Soc. 1 (1999) 181–186, https://doi.org/10.1046/j.1524-475X.1993.10308.x.

[42] A. Shaikh-Kader, N.N. Houreld, N.K. Rajendran, H. Abrahamse, Levels of cyclooxygenase 2, Interleukin-6, and tumour necrosis factor-α in fibroblast cell culture models after Photobiomodulation at 660 nm, Oxidative Med. Cell. Longev. 13 (2021) 6667812, https://doi.org/10.1155/2021/6667812.

[43] K. Rupel, L. Zupin, G. Ottaviani, et al., Blue laser light inhibits biofilm formation in vitro and in vivo by inducing oxidative stress, NPJ Biofilms Microbiomes 9 (2019) 29, https://doi.org/10.1038/s41522-019-0102-9.

[44] F.D. Halstead, M.A. Hadis, N. Marley, et al., Violet-blue light arrays at 405 nanometers exert enhanced antimicrobial activity for photodisinfection of monomicrobial nosocomial biofilms, Appl. Environ. Microbiol. 85 (2019), https://doi.org/10.1128/AEM.01346-19 e01346–19.

[45] I. Plattfaut, E. Demir, P. Fuchs, et al., Characterization of blue light treatment for infected wounds: Antibacterial efficacy of 420, 455 and 480 nm light emitting diodes against common skin pathogens vs. blue light-induced skin cell toxicity, Photobiomodul Photomed Laser Surg 39 (2021) 339–348, https://doi.org/10.1089/photob.2020.4932.

[46] M. Baffoni, L.J. Bessa, R. Grande, et al., Laser irradiation effect on Staphylococcus aureus and Pseudomonas aeruginosa biofilms isolated from venous leg ulcer, Int. Wound J. 9 (2012) 517–524, https://doi.org/10.1111/j.1742-481X.2011.00910.x.

[47] Y.P. Krespi, V. Kizhner, L. Nistico, et al., Laser disruption and killing of methicillin-resistant Staphylococcus aureus biofilms, Am. J. Otolaryngol. 32 (2011) 198–202, https://doi.org/10.1016/j.amjoto.2010.01.010.

[48] W. Posten, D.A. Wrone, J.S. Dover, et al., Low-level laser therapy for wound healing: mechanism and efficacy, Dermatol. Surg. 31 (2005) 334–340, https://doi.org/10.1111/j.1524-4725.2005.31086.

[49] S.M. Rodrigo, A. Cunha, D.H. Pozza, et al., Analysis of the systemic effect of red and infrared laser therapy on wound repair, Photomed. Laser Surg. 27 (2009) 929–935, https://doi.org/10.1089/pho.2008.2306111/j.1524-4725.2005.31086.

[50] E.L. Nussbaum, T. Mazzulli, K.P. Pritzker, et al., Effects of low intensity laser irradiation during healing of skin lesions in the rat, Lasers Surg. Med. 41 (2009) 372–381, https://doi.org/10.1002/lsm.20769.

[51] E.L. Nussbaum, F.L. Heras, K.P. Pritzker, et al., Effects of low intensity laser irradiation during healing of infected skin wounds in the rat, Photonics Lasers Med. 3 (2014) 23–36, https://doi.org/10.1515/plm-2013-0049.

[52] A.M.C.T. Lima, L.P. da Silva Sergio, L.A., da Silva Neto Trajano, et al., Photobiomodulation by dual-wavelength low-power laser effects on infected pressure ulcers, Lasers Med. Sci. 35 (2020) 651–661, https://doi.org/10.1007/s10103-019-02901-6.

[53] T. Briggs, G. Blunn, S. Hislop, et al., Antimicrobial photodynamic therapy-a promising treatment for prosthetic joint infections, Lasers Med. Sci. 33 (2018) 523–532, https://doi.org/10.1007/s10103-017-2394-4.

[54] C. Pérez, T. Zúñiga, C.E. Palavecino, Photodynamic therapy for treatment of Staphylococcus aureus infections, Photodiagn. Photodyn. Ther. 34 (2021), 102285, https://doi.org/10.1016/j.pdpdt.2021.102285.